Transition Structures of Methane Elimination in Pentamethylniobium and Pentamethyltantalum†

Yun-Dong Wu,* Kyle W. K. Chan, and Ziling Xue

Contribution from the Department of Chemistry, Hong Kong University of Science and Technology, Clear Water Bay, Kowloon, Hong Kong, and Department of Chemistry, University of Tennessee, Knoxville, Tennessee 37996-1600

Received February 17, 1995®

Abstract: Intramolecular methane elimination through α-hydrogen abstraction in $M(CH_3)_5$ (M = Nb, Ta) has been studied in detail with *ab initio* quantum mechanics calculations. Geometry optimizations were performed with the 3-21G and HW3 (equivalent to the 6-31G*) basis sets. The energies were further evaluated with the MP2/HW3 calculations. Although the $M(CH_3)_5$ reactants significantly favor square-planar structures, the most favorable transition structure for unimolecular methane elimination is close to a trigonal- bipyramidal geometry. Hydrogen abstraction is concerted, although there is significant M−H interaction in the transition structure. The calculated activation free energy is 35.3 and 37.3 kcal/mol for $Nb(CH_3)_5$ and $Ta(CH_3)_5$, respectively, at the best level of calculation. A dimeric mechanism through intermolecular hydrogen abstraction is found to be much lower in activation free energy than the unimolecular mechanism. The stabilization for the dimeric transition structure is mainly due to the formation of an $M-CH_2-M$ bridge. Intramolecular methane eliminations in $(CH_3)_4M-CH_2-M(CH_3)_4$ were also studied.

The discovery by Schrock of α-hydrogen abstraction in simple alkyl derivatives of high-oxidation-state niobium and tantalum to form alkylidene and alkylidyne derivatives[1-4] has resulted in the development of new fields of organic chemistry: catalytic olefin metathesis[5] and thin-film materials[6] by vapor deposition technique.[7] It is important to understand the factors that determine the stabilities of these compounds and the mode of alkane elimination. For example, $Nb(CH_3)_5$ and $Ta(CH_3)_5$ undergo decomposition readily at −30 °C and room temperature, respectively. The reaction is autocatalytic and gives a non-hydrolyzable metal-containing residue which has the approximate composition $MC_{1.5}H$ with elimination of 3.4 units of methane.[1] More sterically crowded $Ta(CH_2Ph)_5$ is much more stable and decomposes fairly quickly only under elevated temperatures (80 °C).[1] This reaction is apparently in a first-order kinetics and eliminates 2.6 units of toluene from each $Ta(CH_2Ph)_5$.[8] Recently, one of us (Z. Xue) found that the reaction of Ns_3TaCl_2 (Ns = CH_2SiMe_3) with two molecules of LiNs smoothly forms Ns_5Ta.[9] Ns_5Ta decomposes readily with a first-order kinetics to form $Ns_3Ta{=}CHSiMe_3$,[9,10] which further decomposes to give the Wilkinson's compound.[11] It has also been found that the formation of $Np_3Ta{=}CHCMe_3$ (Np = CH_2CMe_3) from neopantane elimination of Np_5Ta is fast at room temperature.[2,9] Here steric effect seems to play a crucial role. Schrock has postulated that when the alkyl group is small, e.g. methyl, elimination is through a rate-determining dimeric intermolecular α-hydrogen abstraction as the first step.[1] When the alkyl becomes bulkier, the dimeric mechanism becomes unfavorable for steric reasons, but a unimolecular mechanism becomes feasible because of a release of steric interactions.

Detailed information of the geometrical and electronic features of these compounds and the transition structure of α-hydrogen abstraction is essential to the understanding of the above seemingly steric effect. Cundari and Gordon have reported *ab initio* calculations on the transition structures of small molecule elimination from group IVB (Ti, Zr, Hf) amido complexes.[12] Their calculations reveal the relative reactivities of these compounds and the features of transition structures. Kang *et al.* recently provided a theoretical explanation for the structures of d° ML_6 and ML_5 complexes.[13] In particular, they studied the structural features of $Ta(CH_3)_5$ in great detail.[13] In agreement with recent experimental determination by Haaland *et al.*,[14] they found a preference of about 9 kcal/mol for a square-pyramidal structure over a trigonal-bipyramidal structure.

In this paper, we report our *ab initio* quantum mechanics study of unimolecular and dimeric methane eliminations of $Nb(CH_3)_5$ and $Ta(CH_3)_5$. In clear support of Schrock's hypothesis, we found that unimolecular methane elimination is

* Address correspondence to this author at the Hong Kong University of Science and Technology.

† Dedicated to Professor Paul von Ragué Schleyer on the occasion of his 65th birthday.

® Abstract published in *Advance ACS Abstracts,* August 15, 1995.

(1) (a) Schrock, R. R. *J. Organomet. Chem.* **1976**, *122*, 209. (b) Schrock, R. R.; Meakin, P. *J. Am. Chem. Soc.* **1974**, *96*, 5288.

(2) Schrock, R. R.; Fellmann, J. D. *J. Am. Chem. Soc.* **1978**, *100*, 3359. Schrock, R. R. *J. Am. Chem. Soc.* **1974**, *96*, 6577, 6796.

(3) (a) Schrock, R. R. *Acc. Chem. Res.* **1979**, *12*, 98. (b) Schrock, R. R. *J. Organomet. Chem.* **1986**, *300*, 249.

(4) For reviews on metal alkyl complexes, see: Davidson, P. J.; Lappert, M. F.; Pearce, R. *Chem. Rev.* **1976**, *76*, 219. Schrock, R. R.; Parshall, G. W. *Chem. Rev.* **1976**, *76*, 244.

(5) For recent reviews see: (a) Schrock, R. R. *Pure Appl. Chem.* **1994**, *66*, 1447. (b) Feldman, J.; Schrock, R. R. In *Progress in Inorganic Chemistry*; Lippard, S. J., Ed.; John Wiley & Sons, Inc.: New York, 1991; Vol. 39. (c) Schrock, R. R. In *Reactions of Coordinated Ligands*; Braterman, P. R., Ed.; Plenum: New York, 1986.

(6) (a) Chisholm, M. H.; Caulton, K. G.; Xue, Z. *Chem. Mater.* **1991**, *3*, 384. (b) Girolami, G. S.; Jensen, J. A.; Pollina, D. M.; Williams, W. S.; Kaloyeros, A. C.; Alloca, C. M. *J. Am. Chem. Soc.* **1987**, *109*, 1579. (c) Duccarriot, M.; Teyssaandir, F. *J. Electrochem. Soc.* **1989**, *136*, 835.

(7) *Mechanisms of Reactions of Organometallics Compounds with Surface*; Cole-Hamilton, D. J., Williams, J. O., Eds.; NATO ASI Series B; Plenum: New York, 1988; Vol. 198.

(8) Malatesta, V.; Ingold, K. U.; Schrock, R. R. J. *Organomet. Chem.* **1978**, *152*, C53.

(9) Li, L.; Xue, Z. *J. Am. Chem. Soc.* Accepted for publication.

(10) Rupprecht, G. A. Ph.D. Thesis, MIT, 1979.

(11) Mowat, W.; Wilkinson, G. *J. Chem. Soc., Dalton* **1973**, 1120.

(12) (a) Cundari, T. R.; Gordon, M. S. *J. Am. Chem. Soc.* **1993**, *115*, 4210. (b) Cundari, T. R. *J. Am. Chem. Soc.* **1992**, *114*, 10557.

(13) Kang, S. K.; Tang, H.; Albright, T. A. J. *Am. Chem. Soc.* **1993**, *115*, 1971. Albright, T. A.; Tang, H. *Angew. Chem.* **1992**, *104*, 1532.

(14) Haaland, A.; Hammel, A.; Rypdal, K.; Verne, H. P.; Volden, H. V.; Pulham, C.; Brunvoll, J.; Weidlein, J.; Greune, M. *Angew. Chem.* **1992**, *104*, 1534.

0002-7863/95/1517-9259$09.00/0

Table 1. Calculated Number of Imaginary Frequency, Zero-Point Energy (ZPE, kcal/mol), Thermal Energy ($\Delta H°_{298}$, kcal/mol), and Entropy (S, cal/(mol·K)) of the Species Involved in $Nb(CH_3)_5$ Decomposition

species	no. of imaginary freq	ZPE	$\Delta H°_{298}$	S
CH_4	0	30.1	31.9	44.4
$Nb(CH_3)_5$ SP (**1**)	0	118.6	126.4	112.1
$Nb(CH_3)_5$ TB (**2**)	3	116.0	123.1	101.4
$Nb(CH_3)_5$ TS (**3**)	1	115.1	122.8	106.2
$Nb(CH_2)(CH_3)_3$ (**4**)	0	84.4	91.2	103.1
$Nb(CH_3)_5$-$Nb(CH_3)_5$ TS (**9**)	1	238.2	253.3	159.9
$Nb(CH_3)_5$-$Nb(CH_3)_5$ TS (**10**)	1	238.5	253.6	159.0
$Nb(CH_3)_5$-$Nb(CH_3)_5$ TS (**11**)	1	237.3	252.8	165.9
$(CH_3)4Nb(CH_2)Nb(CH_3)_4$ (**12**)	0	207.5	221.6	155.9
$(CH_3)4Nb(CH_2)Nb(CH_3)_4$ TS (**13**)	1	205.5	218.8	147.0
$(CH_3)_4Nb(CH_2)Nb(CH_3)_4$ TS (**14**)	1	204.7	218.8	157.1
$(CH_3)_3Nb(CH_2)_2Nb(CH_3)_3$ (**15**)	0	174.5	187.0	146.3
$(CH_3)_4Nb(CH)Nb(CH_3)_3$ (**16**)	0	174.6	187.8	153.3

quite high in activation energy, and a dimeric mechanism has a much lower activation energy. The detailed geometrical features of reactants and transition structures also provide information for the understanding of the steric effect.

Calculation Methods

All calculations were done with the GAUSSIAN 92/DFT program of Pople.[15] For the niobium systems, geometries were fully optimized first with the closed-shell Hartree−Fock method and the all-electron 3-21G basis set of Hehre.[16] Harmonic vibration frequencies were calculated for each structure, based on which thermal energy correction and reaction entropy were calculated. The geometries were further optimized with the HW3 basis set according to Frenking's definition:[17] which was constructed by contraction scheme [3311/2111/311] + ECP on a 28 electron core for the niobium atom[17c] and the 6-31G* basis set for carbon and hydrogen atoms. The energy for each structure was also calculated by the MP2/HW3 method on the HF/HW3 geometries. For the tantalum systems, since the 3-21G basis set for tantalum is not available, geometry optimizations were performed with the HW3 basis set, [3311/2111/211] + ECP on a 60 electron core for the tantalum atom[17d] and the 6-31G* basis set for carbon and hydrogen atoms. This was followed by MP2/HW3 energy calculation. Vibration frequency calculations were not performed for the tantalum systems. Since the geometries of the tantalum systems are very similar to those of the corresponding niobium systems, we have attempted to apply the vibration calculations for the niobium systems to the tantalum systems.

Results and Discussion

The calculated total energies of reactants, transition structures, and products of the unimolecular and dimeric reactions of $Nb(CH_3)_5$ and $Ta(CH_3)_5$ are given in Table 1 of the supporting information. The calculated number of imaginary frequency, zero-point energy (ZPE), thermal energy, and entropy of the species involved in $Nb(CH_3)_5$ decomposition are shown in Table 1. Table 2 gives calculated changes in energies, enthalpies, and entropies of the decomposition reactions.

A. Unimolecular Mechanism. Figures 1 and 2 show the geometries of the reactant, transition structure, and alkylidene product unimolecular methane elimination of $Nb(CH_3)_5$ and Ta-

Table 2. Calculated Changes in Energies (ΔE, kcal/mol) and in the Cases of Niobium Systems Calculated Changes in Enthalpies ($\Delta\Delta H°_{298}$, kcal/mol) and Entropies (ΔS_{298}, cal/(mol·K))

	HF/3-21G			HF/HW3	MP2/HW3//HF/HW3
	ΔE	$\Delta\Delta H°_{298}$	ΔS_{298}	ΔE	ΔE
(1) → **(3)**	54.7	−3.6	−5.9	56.1	37.2
(2) → **(3)**	39.3	-0.3	4.8	45.0	21.2
(1) → **(4)** + CH_4	5.0	−3.2	35.4	2.7	2.4
(5) → **(7)**				57.4	39.2
(6) → **(7)**				51.7	30.5
(5) → **(8)** + CH_4				7.2	5.7
(1) + **(1)** → **(9)**	46.4	0.5	−64.2	53.5	13.2
(1) + **(1)** → **(12)** + CH_4	−10.6	0.8	−23.8	−8.7	−23.6
(12) → **(13)**	50.5	−2.8	−8.9	56.2	26.4
(12) → **(14)**	44.6	−2.8	1.2	46.5	26.2
(12) → **(15)** + CH_4	−9.2	−2.7	34.8	−8.1	−19.5
(12) → **(16)** + CH_4	−8.1	−2.0	41.8	−10.4	−13.7
(5) + **(5)** → **(17)**				53.9	15.5
(5) + **(5)** → **(20)** + CH_4				−9.9	−23.0
(20) → **(21)**				58.3	30.3
(20) → **(22)**				47.8	28.6
(20) → **(23)** + CH_4				−5.0	−13.6
(20) → **(24)** + CH_4				−7.2	−10.7

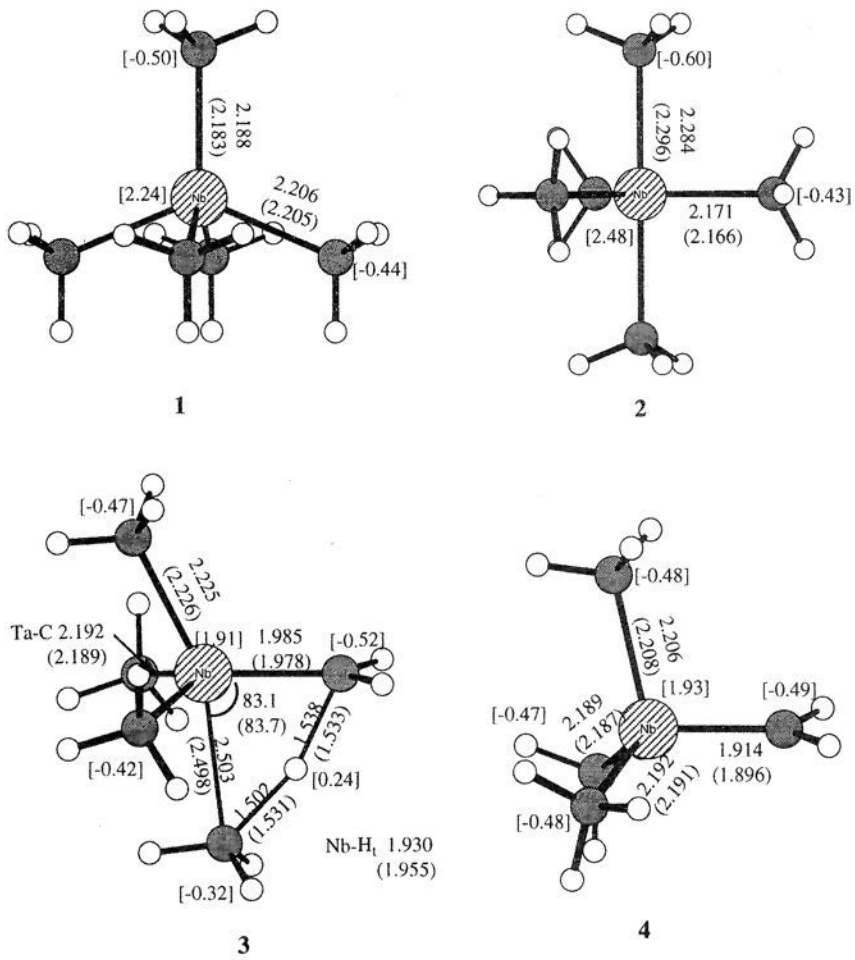

Figure 1. Geometries of the reactant, transition structure, and alkylidene product of unimolecular methane elimination in $Nb(CH_3)_5$ calculated with the 3-21G (in parentheses) and HW3 basis set.

$(CH_3)_5$, respectively. In general, the geometrical parameters for the two systems are very similar, especially the Nb−C and Ta−C bond lengths. This is in agreement with the X-ray crystal structures of Nb and Ta compounds.[18] Therefore, discussions of geometries will be based mainly on the niobium system. The calculated geometries are very similar with the 3-21G and HW3 basis sets as can be seen in Figure 1. In agreement with the results of Kang *et al.* a square-pyramidal structure (**1** and **5**) is most stable for both compounds. A trigonal-bipyramidal structure (**2** and **6**) with a C_3 symmetry constraint has three imaginary vibration frequencies and is 16 and 8.7 kcal/mol less

(15) Gaussian 92/DFT Revision F.2, Frisch, M. J.; Trucks, G. W.; Schlegel, H. B.; Gill, P. M. W.; Johnson, B. G.; Wong, M. W.; Gomperts, R.; Andres, J. L.; Raghavachari, K.; Binkley, J. S.; Gonzalez, C.; Martin, R. L.; Fox, D. J.; Defrees, D. J.; Baker, J.; Stewart, J. J. P.; Pople, J. A., Gaussian, Inc.: Pittsburgh, PA, 1993.

(16) Dobbs, K. D.; Hehre, W. J. *J. Comput. Chem.* **1987**, *8*, 861.

(17) (a) Jonas, V.; Frenking, G.; Reetz, M. T. *J. Comput. Chem.* **1992**, *13*, 919. (b) Jonas, V.; Frenking, G.; Reetz, M. T. *Organometallic* **1993**, *12*, 2111. (c) Hay, P. J.; Wadt, W. R. *J. Chem. Phys.* **1985**, *82*, 299.

(18) (a) Piersol, C. J.; Profilet, R. D.; Fanwick, P. E.; Rothwell, I. P. *Polyhedron* **1993**, *12*, 1779 and references therein. (b) Canahan, E. M.; Lippard, S. J. J. *Am. Chem. Soc.* **1992**, *114*, 4166. (c) Castro, I. D.; Mata, J. D. L.; Gomez, M.; Gomez-Sal, P.; Royo, P.; Selas, J. M. *Polyhedron* **1992**, *11*, 1023.

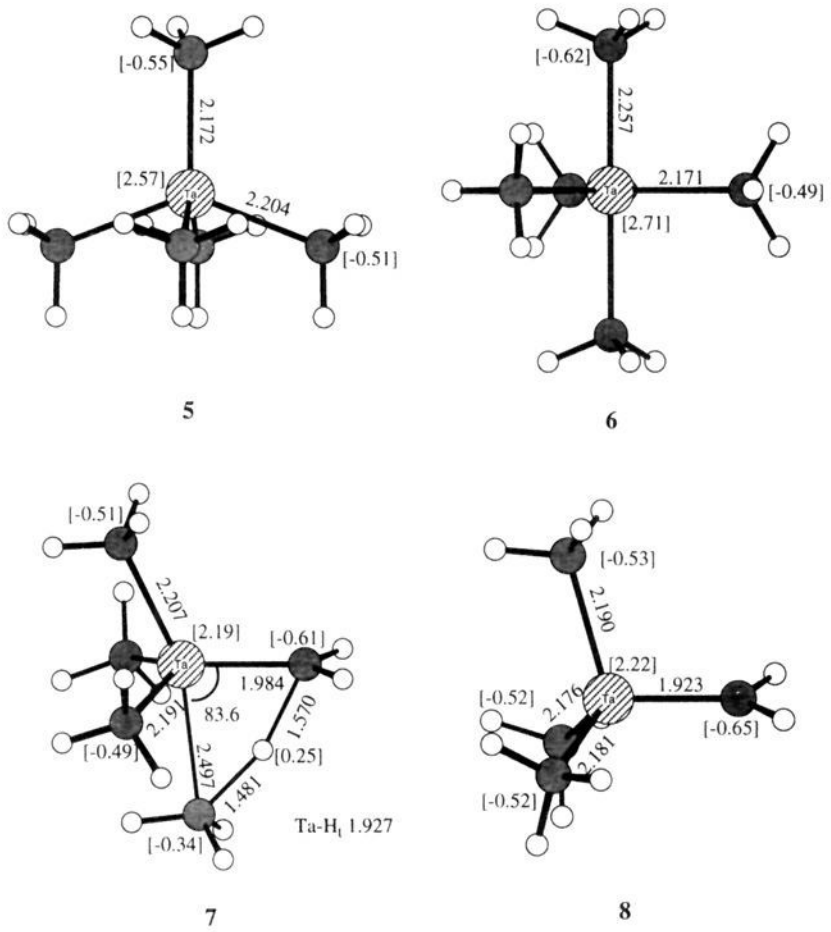

Figure 2. Same as Figure 1 except for $Ta(CH_3)_5$.

stable than the square-pyramidal structures for $Nb(CH_3)_5$ and $Ta(CH_3)_5$, respectively.[19] The preference for the square-pyramidal structures over trigonal-pyramidal has been rationalized by Kang *et al.*[13] When the ligands are not π-donors, as in the current cases, the filled axial L−M−L orbital, which is mainly of p character at the metal in a trigonal-bipyramidal structure, can mix with one of the low-lying empty metal d orbitals as shown by structure **A**. This orbital mixture leads to

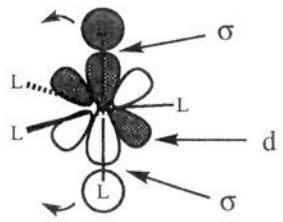

A

a second-order Jahn−Teller distortion to a favorable square-pyramidal structure. Such Jahn−Teller distortion is absent when the ligands are π-donors such as in the cases of VF_5,[20] NbF_5,[21] TaF_5,[21] and $TaBr_5$.[22] Calculated natural atomic charges[23] at Nb and Ta atoms agree with the above argument. The metal atoms in structures **2** and **6** are about 0.24 and 0.15 unit more positively charged than those in structures **1** and **5**, respectively, reflecting the d−p interaction in the square-pyramidal structures.

Only one transition structure can be located for the unimolecular methane elimination for both systems. As shown by structures **3** and **7**, the transition structure is basically a distorted trigonal-bipyramidal structure with the methane elimination from one of the axial positions. The basic features of the transition structure are similar to those found by Cundari *et al.* for small molecule elimination from Ti, Zr, and Hf amido complexes.[12] That is, the breaking M−C bond is about 0.3 Å longer than a normal M−C single bond. The M=C(H_2) bond is almost fully formed, with the carbon center nearly planar. The two partially formed C−H bonds are close to 1.5 Å, which is about 0.1 Å longer than those in the transition structures of hydride transfer reactions,[24] hydrogen abstraction reactions,[25] and pericyclic hydrogen-shift reactions.[26] One factor for this may be the nature of intramolecular hydrogen abstraction which does not allow a smaller C−M−C angle. As will be seen later, the partially formed C−H bonds are shorter in the transition structures of intermolecular hydrogen abstraction (Figure 3). Another factor might be a stabilization of the transferring hydrogen by the metal, referred to as agostic interaction.[27] Based on the Mulliken bond overlap population analysis, Cundari *et al.* suggested that this interaction might be quite significant.[12] The Nb−H and Ta−H in transition structures **3** and **7** are only about 0.14 Å longer than those in $H_3Nb{=}CH_2$ and $H_3Ta{=}CH_2$, respectively.

Schleyer and co-workers reported theoretical studies of degenerate hydrogen transfer between methane and methyllithium[28] and of Zieglar dilithiomethane formation from the decomposition of aggregated methyllithium.[29] They suggest that these reactions are best considered to be hydrogen atom transfer processes since natural population analysis indicates that partial bonds between the transferring hydrogen and the carbon atoms are largely covalent. The charge on the transferring hydrogen atom (+0.26) is only slightly higher than that on the carbon-bound hydrogens (+0.20).[28,29] Similar features are found in the current transition structures. The charge on the transferring hydrogen is about +0.25 as shown in Figures 1 and 2.

The calculated free energy of activation at room temperature (MP2/HW3 energy with 3-21G thermal energy and entropy) with respect to the square-pyramidal structure is 35.3 kcal/mol for $Nb(CH_3)_5$ and 37.3 kcal/mol for $Ta(CH_3)_5$. These activation energies are too high for the reactions to occur at room temperature. Therefore, it can be concluded that methane elimination in $M(CH_3)_5$ does not occur unimolecularly.

The large activation energy for the intramolecular methane elimination is partially due to the geometrical difference between the reactant and transition structure. While the reactant strongly prefers a square-pyramidal structure, the transition structure has to adapt a nearly trigonal-bipyramidal structure. This allows axial methane elimination with the remaining structure in a tetrahedral geometry. A square-pyramidal transition structure could not be located because it would cause too much strain for the formation of the M=C bond.

Based on the above geometrical features, the steric effect on the stability and decomposition mechanism can be qualitatively rationalized. It would be expected that when the alkyl ligands become significantly larger than methyl, for example, CH_2SiMe_3,[9] steric interactions will force the reactant to adapt a trigonal-bipyramidal structure. Therefore, no major geometrical change is needed for intramolecular hydrogen abstraction. Along with the release of steric interactions in the transition

(19) For $Ta(CH_3)_5$, Kang *et al.* reported a distorted trigonal-pyramidal structure which is about 2 kcal/mol more stable than the C_3 symmetrical structure (**6**).

(20) Hagen, K.; Gilbert, M. M.; Hedberg, L.; Hedberg, K. *Inorg. Chem.* **1982**, *21*, 2690.

(21) Petrova, V. N.; Giricher, G. V.; Petrov, V. M.; Goncharuk, V. K. *Zh. Strukt. Khim.* **1985**, *26*, 56.

(22) Ischenko, A. A.; Strand, T. G.; Demidov, A. V.; Spiridonov, V. P. *J. Mol. Struct.* **1978**, *43*, 227.

(23) NBO Version 3.1: Glendening, E. D.; Reed, A. E.; Carpenter, J. E.; Weihold, F. University of Wisconsin, Madison.

(24) Wu, Y.-D.; Houk, K. N. *J. Am. Chem. Soc.* **1987**, *109*, (a) 906, (b) 2226.

(25) Dorigo, A. E.; Houk, K. N. *J. Am. Chem. Soc.* **1987**, *109*, 2195.

(26) Houk, K. N.; Li, Y.; Evanseck, J. D. *Angew. Chem., Int. Ed. Engl.* **1992**, *31*, 682 and references therein.

(27) (a) Schrock, R. R. *Acc. Chem. Res.* **1979**, *12*, 98. (b) Green, M. L. H.; Brookhart, M.; Wong, L. K. *Prog. Inorg. Chem.* **1988**, *36*, 1. (c) Hoffmann, R.; Jemmis, E.; Goddard, R. J. *J. Am. Chem. Soc.* **1980**, *102*, 7667. (d) Bai Y.; Roesky, H.; Noltemeyer, M.; Witt, M. *Chem. Ber.* **1992**, *125*, 825. (e) Cummins, C. C.; van Duyne, G. D.; Schaller, C. P.; Wolczanski, P. T. *Organometallics* **1991**, *10*, 164.

(28) van Eikema Hommes, N. J. R.; Schleyer, P. v. R.; Wu, Y.-D. *J. Am. Chem. Soc.* **1992**, *114*, 1146.

(29) Kaufmann, E.; Schleyer, P. v. R. *J. Comput. Chem.* **1989**, *10*, 437.

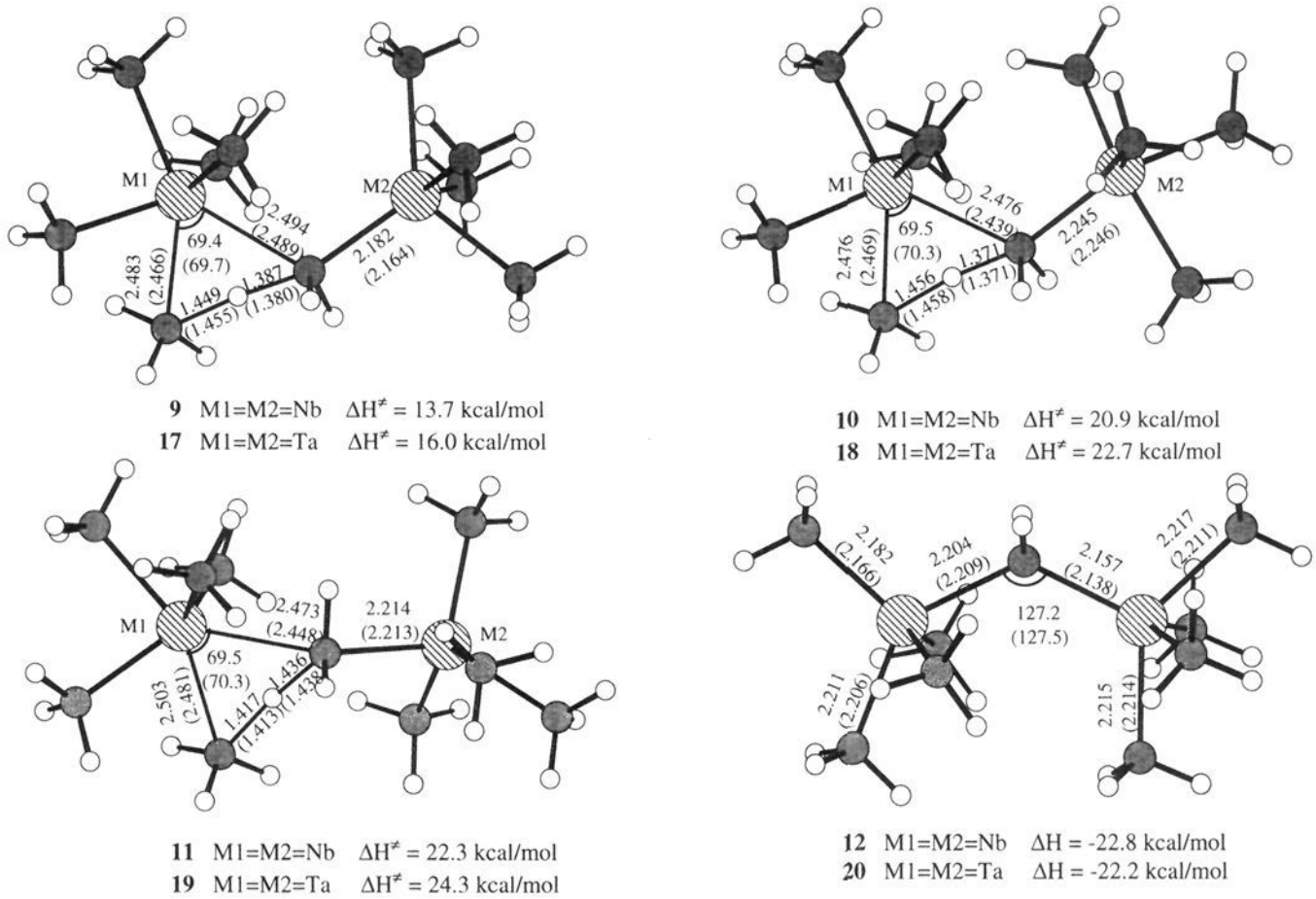

Figure 3. Three transition structures (**9**−**11**, **17**−**19**) and product (**12**, **20**) of the dimeric methane elimination of $Nb(CH_3)_5$ and $Ta(CH_3)_5$. Selected geometrical parameters with the HW3 basis set are given (Ta structures in parentheses).

structure as proposed by Schrock, the activation energy is expected to be much reduced for the unimolecular alkane elimination. This explains why bulky alkyl metal complexes are not stable.[2,9]

The alkylidene products **4** and **8** are nearly tetrahedral.[30] Each structure is slightly distorted from a C_s symmetrical geometry with one of the methyl groups nearly perpendicular to the $M{=}CH_2$ plane. This is similar to the $H_3M{=}CH_2$ (M = Nb, Ta) systems reported by Cunderi *et al.*[31]

B. Dimeric Mechanism. The possible dimeric form for $Nb(CH_3)_5$ was examined with the 3-21G basis set. Starting either from a methyl-bridged structure, $(CH_3)_5Nb\text{- - -}CH_3\text{- - -}Nb(CH_3)_5$, or a structure with full methyl transfer, geometry optimization led to two separated $Nb(CH_3)_5$, apparently due to steric reasons. We conclude that both $Nb(CH_3)_5$ and $Ta(CH_3)_5$ are monomeric in solution.

There are two possible dimeric mechanisms for methane elimination. In one possibility, hydrogen abstraction is intramolecular as discussed above. A second $M(CH_3)_5$ stabilizes the transition structure by metal coordination to the forming CH_2, possibly coupled with an intermolecular methyl transfer, as shown by **B**. In the other possibility, hydrogen abstraction is intermolecular, as shown by mode **C**.

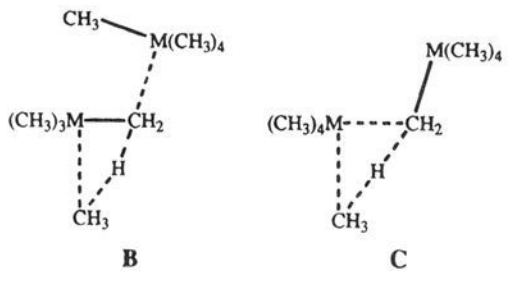

Figure 3 shows three transition structures of dimeric methane elimination (**9**−**11**, **17**−**19**). Each structure is clearly in mode **C**, as indicated by the fact that $C_t{-}M_2$ is shorter than $C_t{-}M_1$. The M_1 center of each structure can be considered as being in a trigonal-bipyramidal conformation in which the $CH_3\text{- - -}H\text{- - -}CH_2$ is just like an axial group. The two partially formed $M_1{-}C$ bonds are of similar length. The $C{-}M_1{-}C$ angle is about 70°, considerably smaller than that in transition structures **3** and **7**. Consequently, the two partially formed C−H bonds are somewhat shorter than those in structures **3** and **7** but are close to those in the reported transition structures of hydride transfer reactions and pericyclic hydrogen shift reactions.[24,26]

The M_2 center of each structure is in a square-pyramidal geometry with the transferring CH_3 either in the axial or an equatorial position, as in $M(CH_3)_5$. In structures **9** and **17** the C_t is axial, while in structures **10**, **18**, **11**, and **19** it is equatorial. Structure **9** is calculated to be more stable than structures **10** and **11** by 7.0 and 9.2 kcal/mol, respectively, and structure **17** is more stable than structures **18** and **19** by 6.4 and 8.8 kcal/mol, respectively. This axial preference is understandable based on both electronic and steric arguments. Electronically, the C_t is the most electronegative of the carbon atoms, and the $C_t{-}Nb$ bond is of double-bond character. Therefore, the $C_t{-}M{-}C$ angles should be larger than the other $C{-}M{-}C$ angles. This can be nicely accommodated when C_t is axial. Sterically, it is most favorable for the largest group to be axial. It is also noted that structures **10** and **18** are more stable than structures **11** and **19** by 2.2 and 2.4 kcal/mol, respectively. While in structures **10** and **18** the $C_t{-}M_2$ is nearly anti to the $C_t{-}H_t$ ($\angle H_t{-}C_t{-}M_2 = 165°$), the M_2 and H_t are adjacent in structures **11** and **19** as indicated by the $H_t{-}C_t{-}M_2$ angle of about 112°.

The calculated activation enthalpy (Table 2, $\Delta E_{MP2/HW3} + \Delta\Delta H°_{298}$) with structures **9** and **17** is 13.7 and 16.0 kcal/mol for $Nb(CH_3)_5$ and $Ta(CH_3)_5$, respectively. These activation enthalpies are significantly lower than those of monomeric methane elimination. This is apparently due to the formation of $M{-}C{-}M$ bridging. It is also reflected in the reaction enthalpies. The calculated enthalpy is −0.9 kcal/mol for the reaction of $Nb(CH_3)_5$ (**1**) to form $Nb(CH_3)_3CH_2$ (**4**) and methane, but it is −22.8 kcal/mol for the dimeric mechanism.

How can we account for the loss of entropy in the dimeric mechanism? The calculated activation entropy with transition structure **9** is −64.2 cal/(mol·K). This contributes significantly

(30) Xue, Z.; Li, L.; Hoyt, L. K.; Diminnie, J. B.; Pollitte, J. L. *J. Am. Chem. Soc.* **1994**, *116*, 2169.

(31) (a) Cundari, T. R.; Gordon, M. S. *J. Am. Chem. Soc.* **1991**, *113*, 5231. (b) Cundari, T. R.; Gordon, M. S. *J. Am. Chem. Soc.* **1992**, *114*, 539.

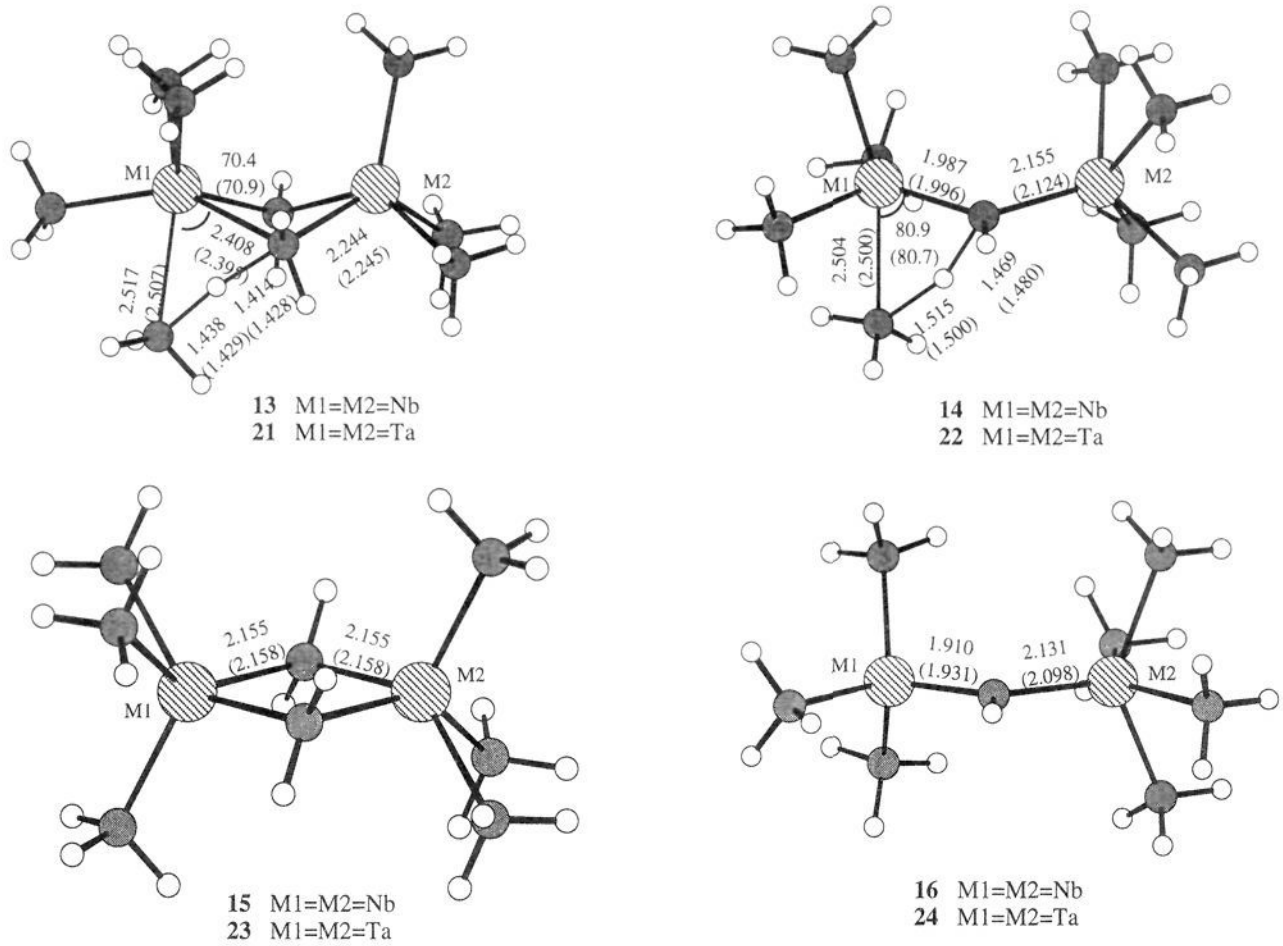

Figure 4. Transition structures and products of intramolecular methane elimination of $(CH_3)_4M-CH_2-M(CH_3)_4$, M = Nb, Ta. Selected geometrical parameters with the HW3 basis set are also given (Ta structures in parentheses).

to the activation free energy. For example, at room temperature, $T\Delta S_{298}$ is 19.1 kcal/mol. This calculated loss of entropy in the transition structure corresponds to the gas phase. Thus, the calculated activation free energy for the dimeric methane elimination of $Nb(CH_3)_5$ in the gas phase is about 32.8 kcal/mol, which is similar to that for the unimolecular mechanism. However, a closer look reveals that the loss of entropy is mainly due to the loss of translation (−39.2 cal/(mol·K)) and rotation (−19.3 cal/(mol·K)). The entropy loss due to the vibration term is only about −5.7 cal/(mol·K). The loss of translation and rotation entropies should be much smaller in solution compared to the gas-phase reaction. Although a quantitative number is difficult to determine by calculations, we expect that the loss of entropy should not contribute significantly to the activation free energy for the two reactions. We conclude that the dimeric methane elimination of $Nb(CH_3)_5$ and $Ta(CH_3)_5$ in solution should have much lower activation energy than the unimolecular mechanism. This supports Schrock's postulation.[1] It also explains why $Ta(CH_3)_5$ is stable in a dilute solution.[1,4]

The calculated activation energy (see Figure 3) for the reaction of two $Nb(CH_3)_2$ is about 2 kcal/mol smaller than that for the reaction of two $Ta(CH_3)_5$. This qualitatively agrees with the fact that $Nb(CH_3)_5$ is less stable than $Ta(CH_3)_5$ and decomposes at lower temperatures.

Structures **12** and **20** are the product from dimeric methane elimination of $Nb(CH_3)_5$ and $Ta(CH_3)_5$, respectively. Each metal center is square pyramidal. The bridging CH_2 is equatorial with respect to M1 and axial with respect to M2. This structure is slightly more stable than a structure with the bridging CH_2 axial with respect to both metal centers. In the later structure there are more steric interactions among the methyl groups on the two metal centers. The two bridging $M-C(H_2)$ bonds are similar to other M−C bonds. The M−C−M angle is about 18° larger than a tetrahedral angle apparently due to steric interactions.

C. Further Decomposition. What would be the mechanism of further decomposition in the formation of $MC_{1.5}H$ residue? As pointed out by Schrock *et al.*, the mechanism must be a complicated one. Three reactions can be considered for the product from dimeric methane elimination. The first is the reaction with another molecule of $M(CH_3)_5$ to form $(CH_3)_4M-CH_2-M(CH_3)_3-CH_2-M(CH_3)_4$. This reaction should have similar reactivity as the dimeric methane elimination that has just been discussed. The second reaction involves methane elimination similar to the dimeric mechanism to form a dibridged structure $(CH_3)_3M(CH_2)_2M(CH_3)_3$. In the third reaction the methane elimination is achieved by intramolecular hydrogen abstraction on the CH_2 bridgehead to form $(CH_3)_3-M-CH-M(CH_3)_4$.

The transition structures and products for the second and third reactions are shown in Figure 4. In structures **13** and **21**, the methane elimination is similar to the intermolecular hydrogen abstraction. The overall structure is similar to structure **9** except for the additional $M1-CH_2-M2$ bridge which exists in the reactant. Thus, the methane elimination is from the axial direction. The $M1(CH_2)_2M2$ unit is a puckered four-membered ring. The calculated activation energy ($\Delta E_{MP2/HW3}$) is 26.4 and 28.6 kcal/mol with structures **13** and **21**, respectively. These activation energies are considerably higher than those calculated for the dimeric methane elimination which are 13.6 and 15.5 kcal/mol. First of all, the formation of the four-membered ring introduces ring strain. Second, also due to the ring structure, the transition structure cannot adapt an ideal geometry as in structures **9** and **17**.

Transition structures **14** and **22** are similar to transition structures **3** and **7** except for the replacement of one $M{=}CH_2$ hydrogen by a $M(CH_3)_4$ group. Thus, the reactive metal center is nearly trigonal-bipyramidal with axial methane elimination. The calculated activation energies for the two structures are about 10 kcal/mol lower than those of transition structures **3** and **7**. The presence of the bystander metal center reduces activation energy because of the M−CH−M conjugation stabilization. This delocalization stabilization is even larger (about 15 kcal/mol) in the products **16** and **24**.

D. Summary. Quantum mechanics *ab initio* calculations have been carried out for the unimolecular and dimeric methane

elimination of $M(CH_3)_5$, M = Nb, Ta. The transition structure for the unimolecular reaction is in a nearly trigonal-bipyramidal geometry. The calculated activation free energy at room temperature for the reaction is about 35 and 37 kcal/mol for M = Nb and Ta, respectively. In agreement with Schrock's hypothesis, this rules out the unimolecular mechanism for the decomposition of $M(CH_3)_5$. The high activation energy is largely due to a strong preference of the reactant for a square-pyramidal geometry. When steric bulkiness is introduced to the alkyl ligands, the activation energy should be reduced because a trigonal-bipyramidal transition structure should have least steric interactions. Dimeric methane elimination through intermolecular hydrogen abstraction is calculated to be much lower in activation energy than unimolecular methane elimination. This is mainly due to the formation of $M-CH_2-M$ bridging in the transition structure and a favorable C−M−C angle (about 70°) for hydrogen transfer.

Acknowledgment. The work was supported by the Hong Kong Research Grant Councel (UST 215/93E), UPGC (DAG92/93.SC10, RI 93/94.SC03), and CCST of HKUST. Z.X. acknowledgs the U.S. National Science Foundation Young Investigator Award (NYI) program, Petroleum Research Fund, the Exxon Education Foundation, and the University of Tennessee (Faculty Research Awards) for support.

Supporting Information Available: Table of calculated energies of reactants, transition structures, and products of the unimolecular and dimeric reactions of $Nb(CH_3)_5$ and $Ta(CH_3)_5$ (1 page). This material is contained in many libraries on microfiche, immediately follows this article in the microfilm version of the journal, can be ordered from the ACS, and can be downloaded from the Internet; see any current masthead page for ordering information and Internet access instructions.

JA950564G